Passenger strand of *miR-145-3p* acts as a tumor-suppressor by targeting *MYO1B* in head and neck squamous cell carcinoma

YASUTAKA YAMADA[1], KEIICHI KOSHIZUKA[1,2], TOYOYUKI HANAZAWA[2], NAOKO KIKKAWA[2], ATSUSHI OKATO[1], TETSUYA IDICHI[3], TAKAYUKI ARAI[1], SHO SUGAWARA[1], KOJI KATADA[2], YOSHITAKA OKAMOTO[2] and NAOHIKO SEKI[1]

Departments of [1]Functional Genomics, [2]Otorhinolaryngology/Head and Neck Surgery, Chiba University Graduate School of Medicine, Chiba 260-8670; [3]Department of Digestive Surgery, Breast and Thyroid Surgery, Graduate School of Medical and Dental Sciences, Kagoshima University, Kagoshima 890-8580, Japan

Received August 31, 2017; Accepted October 23, 2017

DOI: 10.3892/ijo.2017.4190

Abstract. Analysis of the microRNA (miRNA) expression signature of head and neck squamous cell carcinoma (HNSCC) based on RNA sequencing showed that dual strands of pre-*miR-145* (*miR-145-5p*, guide strand; and *miR-145-3p*, passenger strand) were significantly reduced in cancer tissues. In miRNA biogenesis, passenger strands of miRNAs are degraded and have no biological activities in cells. The aims of this study were to investigate the functional significance of the passenger strand of *miR-145* and to identify *miR-145-3p*-regulated oncogenic genes in HNSCC cells. Expression levels of *miR-145-5p* and *miR-145-3p* were significantly downregulated in HNSCC tissues and cell lines (SAS and HSC3 cells). Ectopic expression of *miR-145-3p* inhibited cancer cell proliferation, migration and invasion, similar to *miR-145-5p*, in HNSCC cells. Myosin 1B (*MYO1B*) was directly regulated by *miR-145-3p*, and knockdown of *MYO1B* by siRNA inhibited cancer cell aggressiveness. Overexpression of *MYO1B* was confirmed in HNSCC clinical specimens by analysis of protein and mRNA levels. Interestingly, high expression of *MYO1B* was associated with poor prognosis in patients with HNSCC by analysis of The Cancer Genome Atlas database (p=0.00452). Our data demonstrated that the passenger strand of *miR-145* acted as an antitumor miRNA through targeting *MYO1B* in HNSCC cells. The involvement of dual strands of pre-*miR-145* (*miR-145-5p* and *miR-145-3p*) in the regulation of HNSCC pathogenesis is a novel concept in present RNA research.

Correspondence to: Dr Naohiko Seki, Department of Functional Genomics, Chiba University Graduate School of Medicine, 1-8-1 Inohana Chuo-ku, Chiba 260-8670, Japan
E-mail: naoseki@faculty.chiba-u.jp

Key words: microRNA, microRNA-145-5p, microRNA-145-3p, passenger strand, head and neck squamous cell carcinoma, antitumor, myosin 1B

Introduction

Head and neck squamous cell carcinoma (HNSCC) occurs from the mucosa in the upper aerodigestive tract, including the oral cavity, oropharynx, hypopharynx and larynx, and this disease is the sixth most common cancer worldwide (1). Approximately 550,000 new patients are diagnosed, and 30,000 patients die of this disease annually (2). Due to the local recurrence and distant metastasis of HNSCC, the overall survival of patients with HNSCC has not improved in the last decade (3). Currently developed targeted molecular therapies are not sufficiently efficacious in the management of HNSCC (3). Therefore, improving our understanding of the molecular mechanisms of HNSCC aggressiveness is needed based on current genomic approaches.

MicroRNAs (miRNAs) are small noncoding RNAs (19-22 nucleotides in length) involved in the repression or degradation of target RNA transcripts in a sequence-dependent manner (4). One of the unique features of miRNAs is that a single miRNA regulates a vast number of protein-coding or noncoding RNAs in human cells (5). Thus, aberrant expression of miRNAs disrupts systematically regulated RNA networks in cancer cells. In fact, accumulating evidence has revealed that aberrant expression of miRNAs is deeply involved in the pathogenesis of human cancers (6).

In miRNA biogenesis, precursor miRNA (pre-miRNA) is cleaved in the cytoplasm, generating a miRNA duplex comprised of a guide strand and passenger strand. The guide strand of miRNA is thought to be incorporated into the RNA-induced silencing complex (RISC) to target mRNAs, whereas the passenger strand of miRNA is degraded and is not thought to have regulatory activity in cells (7). However, in contrast to this paradigm, we demonstrated that passenger strands of miRNAs, i.e., *miR-144-5p*, *miR-139-3p*, *miR-150-3p* and *miR-145-3p*, were downregulated and acted as antitumor miRNAs in several types of cancers (8-13). Moreover, dual strands of pre-*miR-145* (*miR-145-5p* and *miR-145-3p*) coordinately target oncogenic

MTDH and *UHRF1* in lung cancer and bladder cancer, respectively (10,11). The involvement of passenger miRNA strands and regulation of cancer networks by passenger miRNAs are novel concepts in cancer research.

Analysis of the miRNA expression signature of HNSCC by RNA sequencing revealed that *miR-145-5p* and *miR-145-3p* were significantly downregulated in cancer tissues. The guide strand *miR-145-5p* has been established as an oncogene in several cancers, including HNSCC (14). However, the functional significance of the passenger strand of *miR-145* in HNSCC is still unknown. The aims of this present study were to investigate the antitumor function of *miR-145-3p* and to identify its target oncogenic genes in HNSCC cells. Elucidation of the antitumor roles of passenger strands of miRNAs and the cancer networks mediated by these miRNAs may provide insights into the molecular pathogenesis of HNSCC.

Materials and methods

Clinical HNSCC specimens, cell lines, and cell culture. A total of 22 clinical tissue specimens were collected from patients with HNSCC who underwent surgical resection at Chiba University Hospital between 2008 and 2014. The clinicopathological features of patients with HNSCC are summarized in Table I. All patients in this study provided informed consent, and the study protocol was approved by the Institutional Review Board of Chiba University. TNM classification and tumor stage were determined by the Union for International Cancer Control (UICC) (15).

In this study, we used the following human HNSCC cells: SAS (derived from a primary lesion of tongue squamous cell carcinoma) and HSC3 (derived from human lymph node metastasis of tongue squamous cell carcinoma), as described previously.

Mature miRNA and small interfering RNA (siRNA) transfection into HNSCC cells. The following RNA species were used in this study: mature miRNAs, Pre-miR miRNA Precursors (*hsa-miR-145-3p*, assay ID: PM 13036; *hsa-miR-145-5p*, assay ID: PM 11480), negative control miRNA (assay ID: AM 17111) (both from Applied Biosystems, Foster City, CA, USA), siRNA (Stealth Select RNAi siRNA; si-*MYO1B* P/N: HSS106714 and HSS106716; Invitrogen, Carlsbad, CA, USA). The transfection procedures were described previously (16-20).

Quantitative real-time reverse transcription polymerase chain reaction (qRT-PCR). The procedure for PCR quantification was described previously (16-19). TaqMan probes and primers for *MYO1B* (P/N: Hs00362654_m1; Applied Biosystems) were assay-on-demand gene expression products. Expression for *miR-145-3p* (P/N: 002149; Applied Biosystems) and *miR-145-5p* (P/N: 002278) was used to quantify the expression levels of miRNAs according to the manufacturer's protocol. To normalize the data for quantification of mRNA and miRNAs, we used human *GUSB* (P/N: Hs99999908_m1), glyceraldehyde 3-phosphate dehydrogenase (*GAPDH*) (P/N: Hs02758991_m1) and *RNU48* (assay ID: 001006) (all from Applied Biosystems). The relative expression levels were analyzed using the $2^{-\Delta\Delta CT}$ method.

Cell proliferation, migration, and invasion assays. Cell proliferation, migration and invasion assays were described previously (16-19).

Incorporation of miR-145-3p or miR-145-5p into the RISC by Ago2 immunoprecipitation. SAS cells were transfected with 10 nM miRNA by reverse transfection. After 48 h, immunoprecipitation was performed using a human Ago2 miRNA isolation kit (Wako, Osaka, Japan) according to the manufacturer's protocol. Expression levels of *miR-145-3p* or *miR-145-5p* were measured by qRT-PCR. miRNA data were normalized to the expression of miR-150-5p (P/N: PM10070; Applied Biosystems), which was not affected by *miR-145-3p* and *miR-145-5p* transfection.

Western blot analysis. Cells were harvested and lysed 48 h after transfection. Each cell lysate (50 μg of protein) was separated using Mini-PROTEAN TGX gels (Bio-Rad, Hercules, CA, USA) and transferred to polyvinylidene difluoride membranes. Immunoblotting was performed with monoclonal anti-*MYO1B* antibodies (1:250 dilution; HPA013607; Sigma-Aldrich, St. Louis, MO, USA). Anti-glyceraldehyde 3-phosphate dehydrogenase (GAPDH) antibodies (1:1,000 dilution; ab8245; Abcam, Cambridge, UK) were used as an internal control. The procedures were described in our previous studies (16-19).

Identification of putative genes regulated by miR-145-3p in HNSCC cells. Specific genes regulated by *miR-145-3p* were identified by a combination of *in silico* and genome-wide gene expression analyses. Genes regulated by *miR-145-3p* were listed using the TargetScan database. Oligo microarrays (Human GE 60K; Agilent Technologies) were used for gene expression analyses. The microarray data were deposited into GEO (http://www.ncbi.nlm.nih.gov/geo/), with accession number GSE82108. Upregulated genes in HNSCC were obtained from publicly available data sets in GEO (accession no. GSE9638). To identify signaling pathways regulated *in silico*, gene expression data were analyzed using the KEGG pathway categories with the GeneCodis program.

Regulation of targets downstream of MYO1B in HNSCC. We investigated pathways regulated by *MYO1B* in HNSCC cells. We analyzed gene expression using si-*MYO1B*-transfected SAS cells. Microarray data were used for expression profiling of si-*MYO1B* transfectants. The microarray data were deposited into GEO (accession no. GSE100746). We analyzed common downregulated genes using the GEO dataset.

Plasmid construction and dual-luciferase reporter assay. The partial wild-type sequence of the *MYO1B* 3'-untranslated region (3'-UTR) was inserted between the *Xho*I-*Pme*I restriction sites in the 3'-UTR of the hRluc gene in the psiCHECK-2 vector (C8021; Promega, Madison, WI, USA). Alternatively, we used sequences that were missing the *miR-145-3p* target sites (position 88-94 or position 1117-1123). The synthesized DNA was cloned into the psiCHECK-2 vector. SAS cells were transfected with 20 ng of the vector, 20 nM microRNAs, and 1 μl Lipofectamine 2000 in 100 μl Opti-MEM (both from Invitrogen). The procedure of dual-luciferase reporter assay was described previously (16-19).

Table I. Clinical features of 22 patients with HNSCC.

No.	Age	Sex	Location	T	N	M	Stage	Differentiation
1	64	F	Oral floor	4a	2c	0	IVA	Moderate
2	73	M	Tongue	3	2b	0	IVA	Poor
3	77	M	Tongue	2	2b	0	IVA	Poor
4	63	F	Oral floor	2	2b	0	IVA	Basaloid SCC
5	59	M	Tongue	1	2a	0	IVA	Moderate
6	36	F	Tongue	3	1	0	III	Moderate
7	67	M	Tongue	3	0	0	III	Moderate
8	60	F	Tongue	2	1	0	III	Well
9	66	M	Tongue	2	0	0	II	Moderate
10	67	M	Tongue	2	0	0	II	Poor to moderate
11	76	F	Tongue	1	0	0	I	Well
12	69	M	Tongue	1	0	0	I	Well
13	73	F	Tongue	1	0	0	I	Well
14	64	M	Tongue	1	0	0	I	Well
15	70	M	Tongue	1	0	0	I	Well
16	38	M	Tongue	1	0	0	I	Well
17	51	M	Tongue	1	0	0	I	Well
18	34	F	Tongue	1	0	0	I	Poor
19	70	M	Tongue	1	0	0	I	Moderate
20	71	M	Tongue	1	0	0	I	Well
21	82	M	Oral floor	1	0	0	I	Well
22	81	M	Tongue	1	0	0	I	Extremely well

HNSCC, head and neck squamous cell carcinoma; F, female; M, male; TNM classification and tumor stage were determined by the Union for International Cancer Control (UICC).

Immunohistochemistry. Formalin-fixed, paraffin-embedded (FFPE) tissues were used. Tissue sections were incubated overnight at 4˚C with anti-*MYO1B* antibodies diluted 1:300 (HPA013607; Sigma-Aldrich). The procedure for immunohistochemistry was described previously (21).

The Cancer Genome Atlas (TCGA)-HNSCC data analysis. To explore the clinical significance of *MYO1B* in HNSCC, we used the RNA sequencing database in TCGA (https://tcga-data.nci.nih.gov/tcga/). The gene expression and clinical data were retrieved from cBioportal (http://www. cbioportal.org/, the provisional data downloaded July 1, 2017).

Statistical analysis. Relationships between two or three variables and numerical values were analyzed using Mann-Whitney U tests or Bonferroni-adjusted Mann-Whitney U tests. Spearman's rank tests were used to evaluate the correlations between the expression of *miR-145-3p* or *miR-145-5p* and target genes. Expert StatView software (version 5.0; SAS Institute Inc., Cary, NC, USA) was used for these analyses. Multivariate Cox proportional hazard regression models were used to determine independent factors for survival with JMP Pro 13.

Results

Expression levels of miR-145-5p and miR-145-3p in HNSCC clinical specimens and cell lines. To confirm our miRNA expression signatures in HNSCC by RNA sequencing, we validated the expression levels of *miR-145-5p* and *miR-145-3p* in HNSCC clinical specimens and cell lines. In Fig. 1, the expression levels of *miR-145-5p* and *miR-145-3p* were significantly reduced in cancer tissues compared with those in corresponding adjacent noncancerous epithelium ($p<0.0001$) (Fig. 1A). Additionally, the expression levels of *miR-145-5p* and *miR-145-3p* in SAS and HSC3 cells were markedly downregulated (Fig. 1A).

Spearman's rank test showed a positive correlation between the expression levels of *miR-145-5p* and *miR-145-3p* in clinical specimens (Fig. 1A).

Effects of ectopic expression of miR-145-5p and miR-145-3p on cell proliferation, migration and invasion in HNSCC cell lines. To validate the functional roles of *miR-145-3p* and *miR-145-5p*, we carried out gain-of-function assays using miRNA transfection into two HNSCC cell lines (SAS and HSC3). XTT assays revealed that cell proliferation was significantly inhibited in *miR-145-3p* and *miR-145-5p* transfectants in comparison with mock or miR-control transfectants (Fig. 1B). Similarly, migration assays showed that cell migration activity was significantly inhibited in *miR-145-3p* and *miR-145-5p* transfectants in comparison with mock and miR-control transfectants (Fig. 1C). Matrigel invasion assays also demonstrated that cell invasion activity was significantly inhibited in *miR-145-3p* and *miR-145-5p*

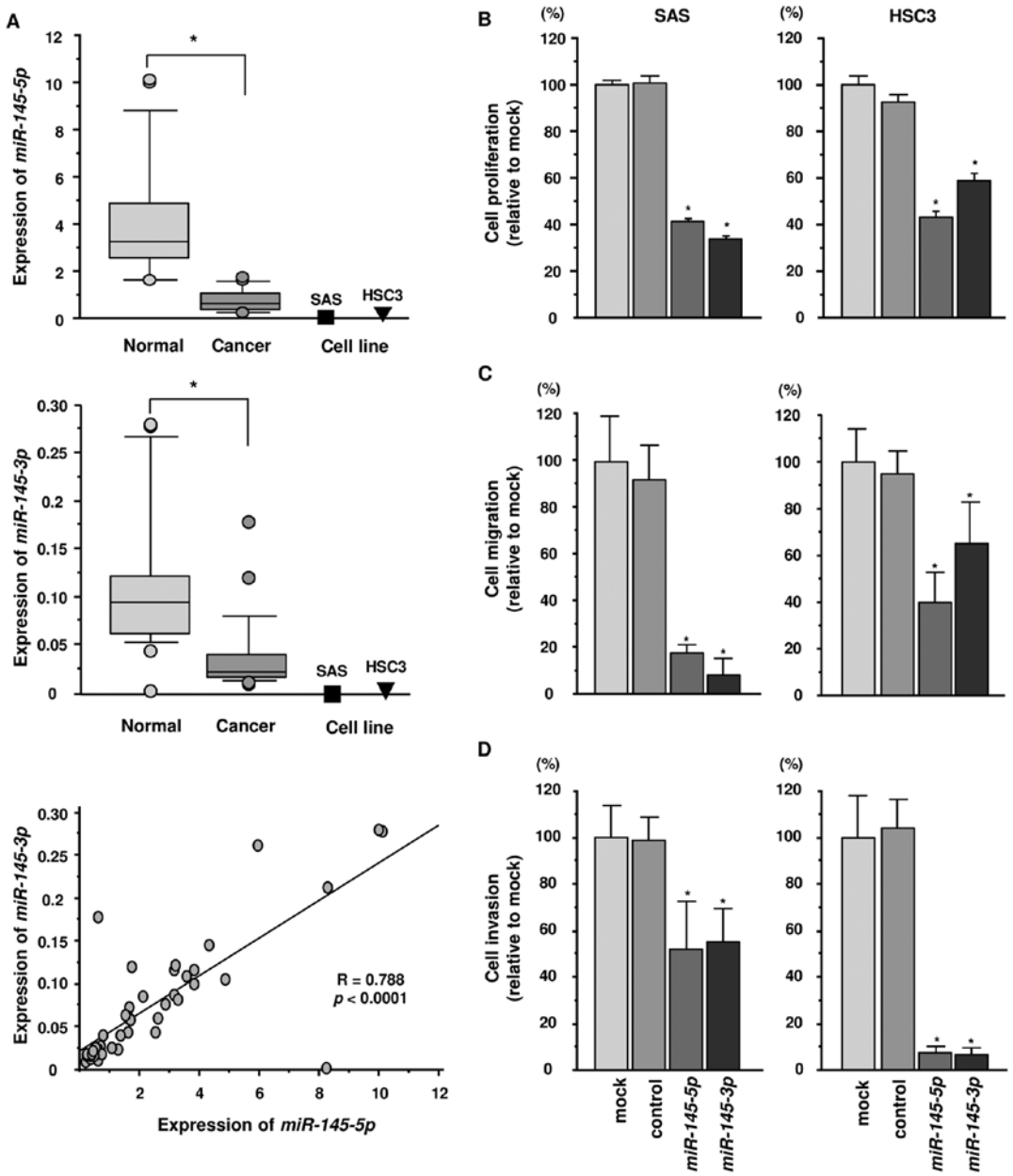

Figure 1. Antitumor function of *miR-145-5p* and *miR-145-3p* in head and neck squamous cell carcinoma (HNSCC) cells. (A) Expression levels of *miR-145-5p* and *miR-145-3p* in HNSCC clinical specimens and cell lines. *RNU48* was used as an internal control. Spearman's rank test showed a positive correlation between the expression of *miR-145-5p* and *miR-145-3p*. *p<0.0001. (B) Cell proliferation was determined by XTT assays 72 h after transfection with *miR-145-5p* and *miR-145-3p*. *p<0.0001. (C) Cell migration activity was determined using migration assays. *p<0.0001. (D) Cell invasion activity was determined using Matrigel invasion assays. *p<0.0001.

transfectants in comparison with mock and miR-control transfectants (Fig. 1D).

Incorporation of miR-145-3p into the RISC in HNSCC cells. We hypothesized that the passenger strand *miR-145-3p* may be incorporated into the RISC and exert important effects in cancer cells. Accordingly, we performed immunoprecipitation with antibodies targeting Ago2, which plays an important role in the RISC. After transfection with *miR-145-3p* or *miR-145-5p*, Ago2-bound miRNAs were isolated, and qRT-PCR was carried out to determine whether *miR-145-3p* and *miR-145-5p* bound to Ago2. After transfection with *miR-145-3p* and immunoprecipitation by anti-Ago2 antibodies, *miR-145-3p* levels were significantly higher than those of mock- or miR-control-transfected cells and those of *miR-145-5p*-transfected SAS cells (p<0.0001) (Fig. 2A). Similarly, after *miR-145-5p* transfection, *miR-145-5p* was detected by Ago2 immunoprecipitation (p<0.0001) (Fig. 2B).

Identification of putative targets of miR-145-3p regulation in HNSCC cells. We performed *in silico* and gene expression analyses to identify genes targeted by *miR-145-3p* for regulation (Fig. 3). First, we selected putative *miR-145-3p* target genes using the TargetScan database and identified 3,164 genes. Next, we performed comprehensive gene expression analysis using *miR-145-3p* transfectants of SAS, with negative control miRNA transfectants serving as controls (accession no. GSE 82108). A total of 1,187 genes were

Table II. Putative targets of *miR-145-3p* regulation in HNSCC cells.

Gene symbol	Gene name	Conserved site count	SAS *miR-145-3p* transfection	HNSCC fold-change	Prognosis (high vs. low) p-value
MYO1B	Myosin IB	2	-1.49	1.72	0.00452
C16orf74	Chromosome 16 open reading frame 74	1	-0.88	1.97	0.014
SP9	Sp9 transcription factor	1	-0.97	2.38	0.0277[a]
RBP1	Retinol binding protein 1, cellular	1	-1.2	2.6	0.0316
LRRC3	Leucine rich repeat containing 3	2	-0.86	1.54	0.0749
PSPH	Phosphoserine phosphatase	1	-0.8	1.95	0.0804
CDCA7L	Cell division cycle associated 7-like	1	-0.88	1.71	0.107
CBS	Cystathionine-β-synthase	2	-1.29	1.54	0.228
SH2D5	SH2 domain containing 5	1	-1.87	2.34	0.301
PXDN	Peroxidasin homolog (*Drosophila*)	1	-0.94	1.63	0.317
CYP27B1	Cytochrome P450, family 27, subfamily B, polypeptide 1	2	-0.86	2.65	0.531
TNK2	Tyrosine kinase, non-receptor, 2	1	-1.08	2.3	0.789
ALDH1L2	Aldehyde dehydrogenase 1 family, member L2	1	-1.19	2.3	0.855
CCDC103	Coiled-coil domain containing 103	1	-1.77	2.03	0.986

HNSCC, head and neck squamous cell carcinoma; [a]poor prognosis with low expression.

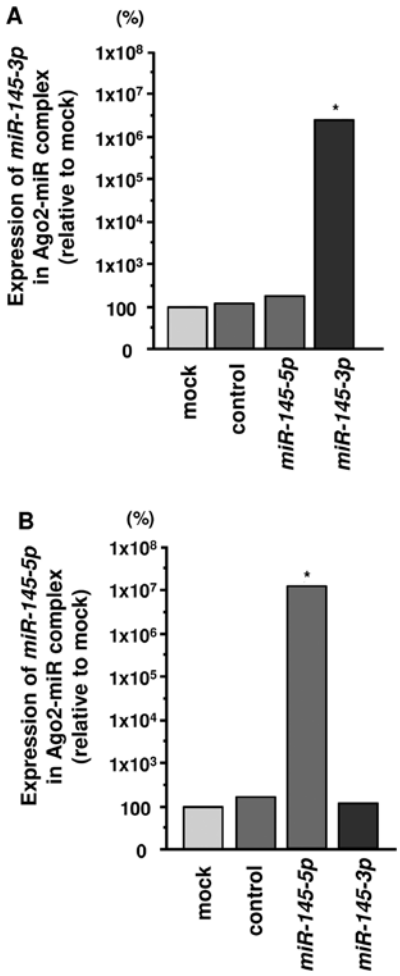

Figure 2. Both strands of *miR-145-5p* and *miR-145-3p* were incorporated into the RISC. (A and B) Expression levels of *miR-145-5p* and *miR-145-3p* after transfection with *miR-145-5p* or *miR-145-3p* following immunoprecipitation by Ago2 (*p<0.0001).

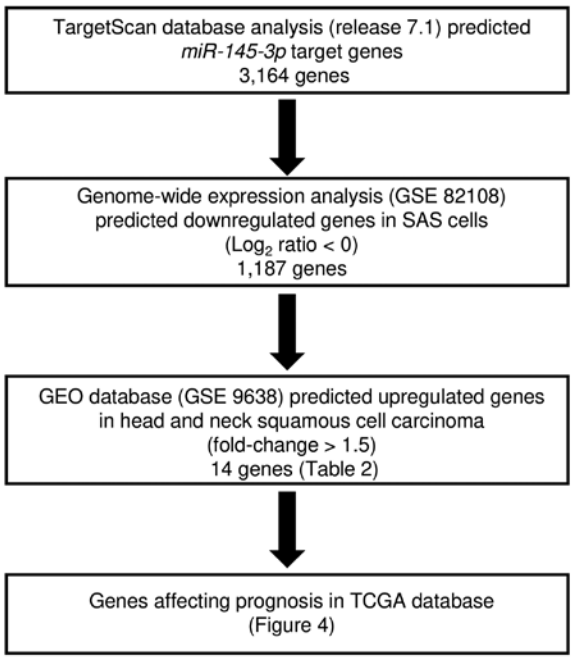

Figure 3. Flow chart illustrating the analysis strategy for *miR-145-3p* targets in head and neck squamous cell carcinoma (HNSCC) cells. A total of 3,164 genes were putative target genes of *miR-145-3p* in TargetScan database analysis (release 7.1). Finally, 14 genes were selected as putative targets of *miR-145-3p* in HNSCC cells.

commonly downregulated ($\log_2$ ratio<0). The gene set was then analyzed with a publicly available gene expression data set in GEO (accession no. GSE9638), and genes upregulated in HNSCC were chosen (fold-change >1.5). A total of 14 genes were identified as candidate targets of *miR-145-3p* regulation (Table II). Next, these genes were validated with TCGA database, and we investigated the correlations between survival

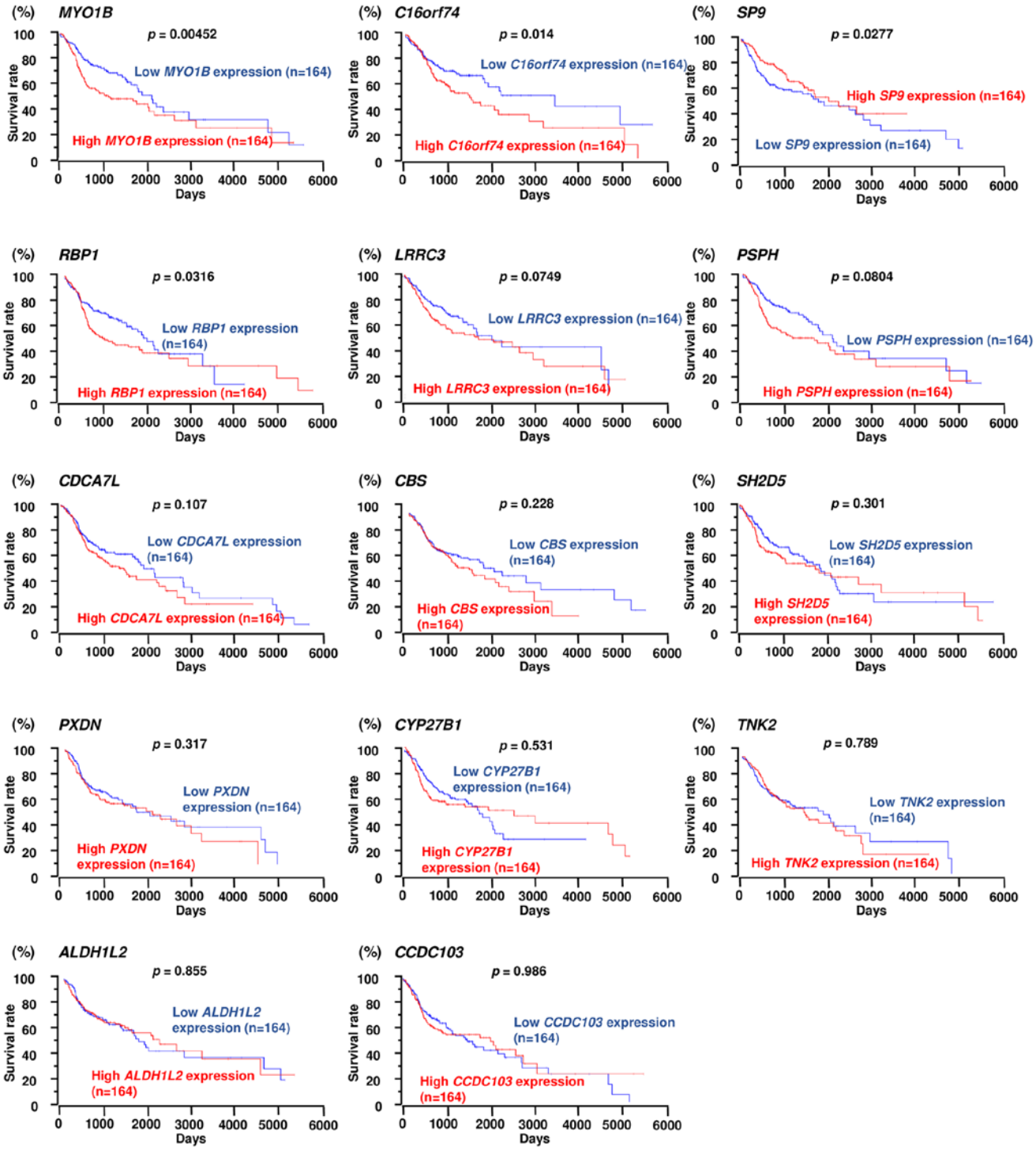

Figure 4. The Cancer Genome Atlas (TCGA) database analysis of putative targets of *miR-145-3p* in head and neck squamous cell carcinoma (HNSCC). Kaplan-Meier plots of overall survival with log-rank tests for 14 genes with high and low expression in the HNSCC TCGA database.

rates and target genes with high or low expression. In this study, 3 genes (*MYO1B*, *C16orf74* and *RBP1*) were selected as genes that affected the patient's overall survival (Table II and Fig. 4). Among them, *MYO1B* was found to have the greatest effect on the overall survival rate (p=0.00452). In this study, we focused on *MYO1B* as a candidate target gene of *miR-145-3p* regulation and investigated the functional roles of HNSCC cells.

Direct regulation of MYO1B by miR-145-3p in HNSCC cells. Next, we investigated whether the expression of *MYO1B* decreased in *miR-145-3p*-transfected HNSCC cells. *MYO1B* mRNA levels were significantly reduced by *miR-145-3p* transfection compared with the mock or miR-control transfectants (Fig. 5A). Furthermore, *MYO1B* protein levels were also reduced by *miR-145-3p* transfection compared with mock or miR-control transfectants (Fig. 5B). In contrast, *miR-145-5p* transfectants did not show altered expression of MYO1B mRNA or protein (Fig. 5A and B).

We then carried out luciferase reporter assays with a vector that included the 3'-UTR of *MYO1B* to confirm that *miR-145-3p*

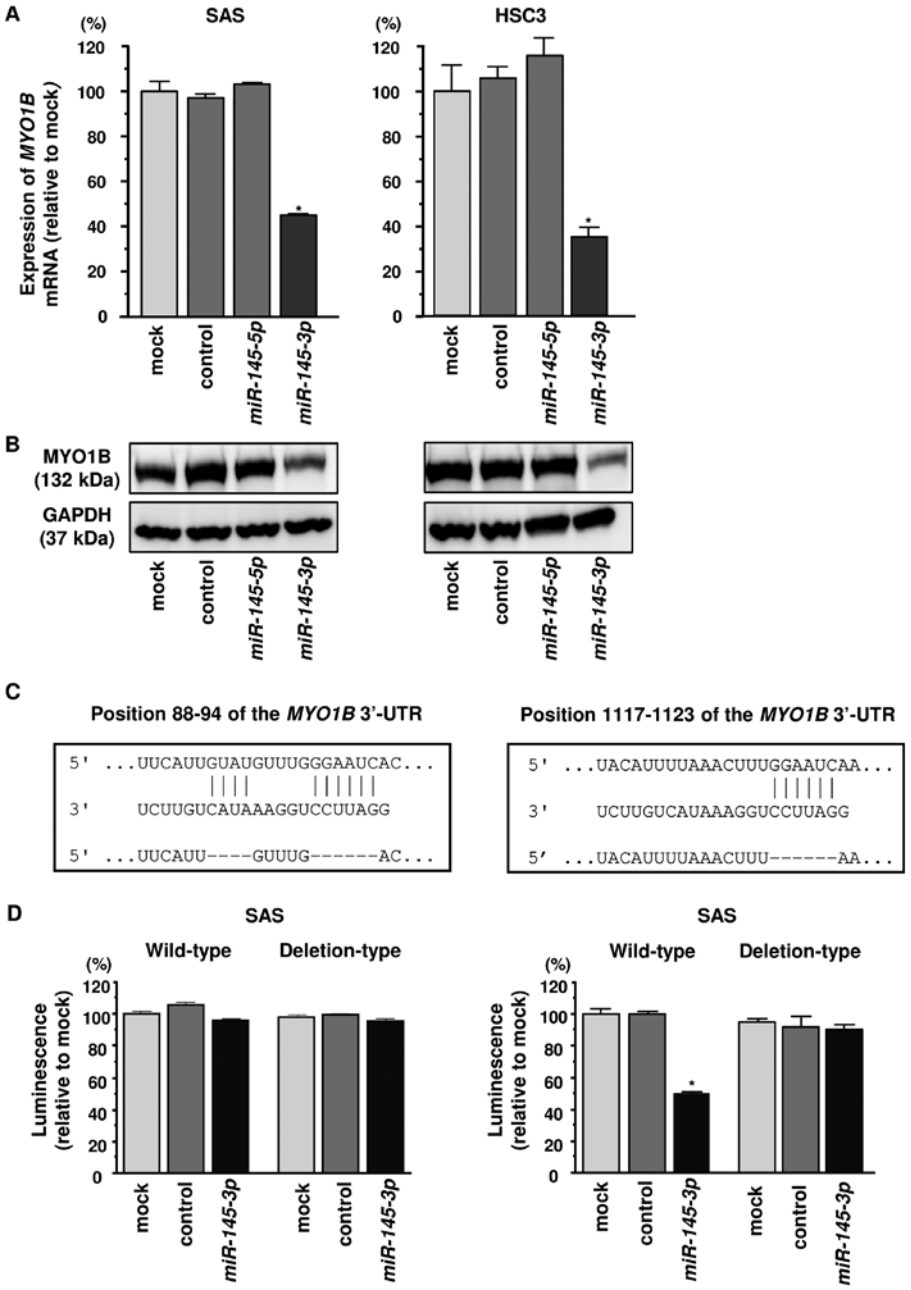

Figure 5. Regulation of myosin 1B (*MYO1B*) expression by *miR-145-3p* in head and neck squamous cell carcinoma (HNSCC) cells. (A) Expression levels of *MYO1B* mRNA 48 h after transfection with 10 nM *miR-145-5p* or *miR-145-3p* into cell lines. *GUSB* was used as an internal control. *p<0.0001. (B) Protein expression of *MYO1B* 72 h after transfection with *miR-145-5p* or *miR-145-3p*. GAPDH was used as a loading control. (C) *miR-145-3p* binding sites in the 3'-untranslated region (3'-UTR) of *MYO1B* mRNA. (D) Dual luciferase reporter assays using vectors encoding putative *miR-145-3p* target sites (positions 88-94 or 1117-1123) in the *MYO1B* 3'-UTR for both wild-type and deleted regions. Normalized data were calculated as the ratio of *Renilla*/Firefly luciferase activities. *p<0.0001.

directly regulated *MYO1B* in a sequence-dependent manner. TargetScan Human database predicted that there were two binding sites for *miR-145-3p* in the 3'-UTR of *MYO1B* (positions 88-94 and 1117-1123) (Fig. 5C). Cotransfection with *miR-145-3p* and vectors significantly reduced luciferase activity in comparison with those in mock and miR-control transfectants in position 1117-1123 of the *MYO1B* 3'-UTR (Fig. 5D).

Effects of MYO1B knockdown on cell proliferation, migration, and invasion in HNSCC cell lines. A loss-of-function assay using siRNA was performed to examine the function of *MYO1B* in HNSCC cell lines. The expression levels of *MYO1B* mRNA and protein were reduced by si-*MYO1B* in HNSCC cell lines (Fig. 6A and B). Furthermore, we investigated effects of *MYO1B* knockdown on cell proliferation, migration, and invasion in HNSCC cell lines. Cancer cell proliferation was significantly reduced in si-*MYO1B* transfectants in comparison with that in mock- or miR control-transfected cell lines (Fig. 6C). Additionally, migration activities were significantly suppressed in si-*MYO1B* transfectants in comparison with that in mock- or miR control-transfected cell lines (Fig. 6D). Invasion activity was also significantly inhibited in si-*MYO1B* transfectants in comparison with that in mock- or miR control-transfected cell lines (Fig. 6E).

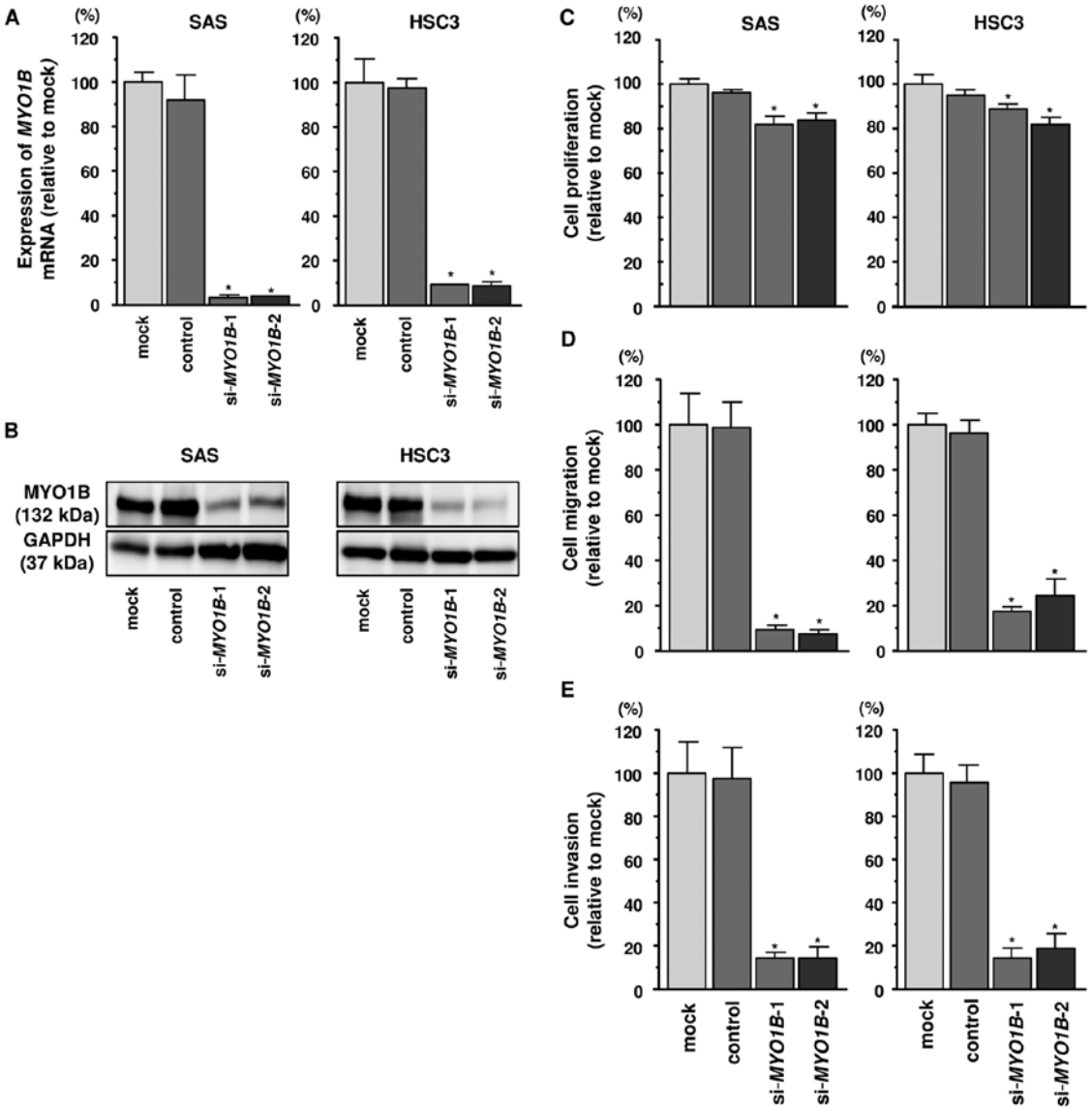

Figure 6. Effects of myosin 1B (*MYO1B*) silencing in head and neck squamous cell carcinoma (HNSCC) cell lines. (A) *MYO1B* mRNA expression 72 h after transfection with 10 nM si-*MYO1B* into HNSCC cell lines. *GUSB* was used as an internal control. *p<0.0001. (B) Protein expression 72 h after transfection with si-MYO1B. GAPDH was used as a loading control. (C) Cell proliferation was determined with XTT assays 72 h after transfection with 10 nM si-*MYO1B*-1 or si-*MYO1B*-2. *p<0.0001. (D) Cell migration activity was determined by migration assays. *p<0.0001. (E) Cell invasion activity was determined using Matrigel invasion assays. *p<0.0001.

Expression of MYO1B in HNSCC clinical specimens. Next, we investigated the mRNA expression levels of *MYO1B* in 22 HNSCC clinical specimens by qRT-PCR. *MYO1B* was significantly upregulated in HNSCC tumor tissues (Fig. 7A). Spearman's rank test showed a negative correlation between the expression of *MYO1B* and *miR-145-3p* (p=0.0025, R=-0.461) (Fig. 7B). Furthermore, we also examined the expression levels of *MYO1B* in HNSCC clinical specimens by immunostaining. *MYO1B* was strongly expressed in several cancer tissues (Fig. 7C: 1, patient no. 2; 2, no. 3; 3, no. 7 in Table I).

Correlation between MYO1B expression and clinicopathological characteristics in prognostic prediction in HNSCC specimens. We collected clinical data from TCGA database and analyzed clinicopathological factors and expression of *MYO1B* as a prognostic predictive factor. The multivariate cox proportional hazards model was used to validate independent predictors for overall survival, including *MYO1B* expression, clinical T stage, clinical N stage, age, sex and histologic grade. As a result, high expression of *MYO1B* was an independent predictive factor for survival [hazard ratio (HR), 1.68; 95% confidence interval (CI), 1.13-2.49; p=0.01] (Fig. 8).

Downstream genes affected by silencing of MYO1B in SAS cells. Finally, we performed genome-wide gene expression analysis using si-*MYO1B* in SAS cells to investigate which genes were mediated by *MYO1B* signaling. A SurePrint G3 Human GE 60K v3 microarray was used for genome-wide expression analysis. We submitted the raw data to the GEO database (accession no. GSE100746). In this study, we focused on significantly downregulated genes by both si-*MYO1B*-1 and si-*MYO1B*-2 transfection ($\log_2$ [si-*MYO1B*/mock] <-1.5). *MYO1B* was the most significantly downregulated gene, indicating that the array data were worthy of evaluation. Genes

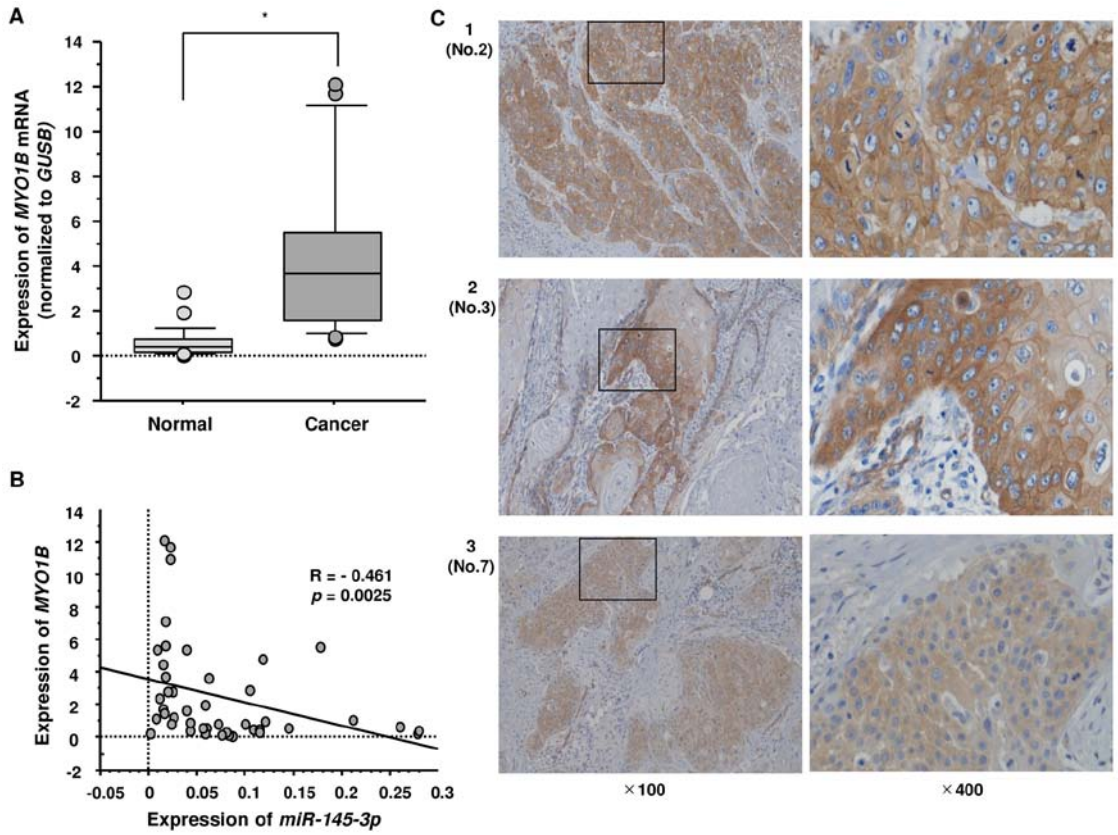

Figure 7. Expression of myosin 1B (*MYO1B*) in clinical specimens of head and neck squamous cell carcinoma (HNSCC). (A) Expression levels of *MYO1B* in HNSCC clinical specimens. *GUSB* was used as an internal control. *p<0.0001. (B) The negative correlation between MYO1B expression and *miR-145-3p* (r=-0.461 and p=0.0025). Spearman's rank test was used to evaluate the correlation. (C) Immunostaining showed that MYO1B was strongly expressed in cancer lesions (x100 and x400 magnification field).

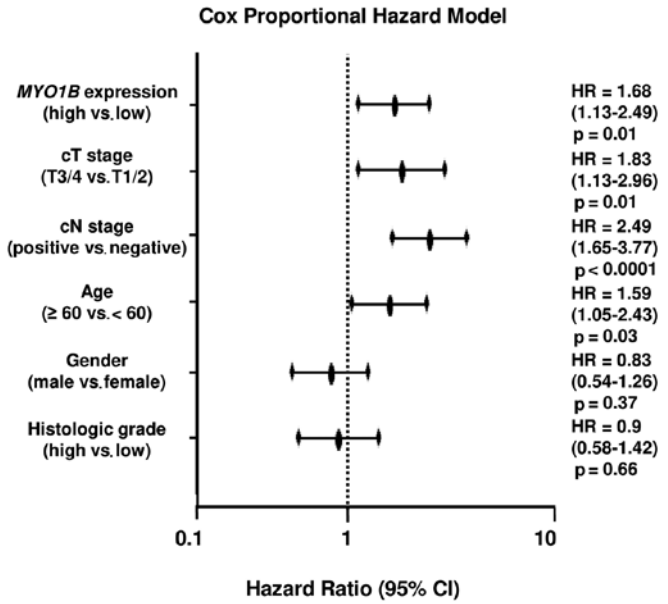

Figure 8. Multivariate Cox proportional hazard regression models for overall survival. Multivariate Cox proportional hazards model for prediction of overall survival showed that high myosin 1B (*MYO1B*) expression, cT stage, cN stage, and age were significant prognostic factors (p=0.01, p=0.01, p<0.0001 and p=0.03, respectively).

significantly downregulated by silencing of *MYO1B* are listed in Table III. Among *MYO1B* downstream genes, expression of 5 genes (*ANXA10*, *TRIM9*, *TCTN3*, *BTBD16* and *CYP19A1*) was significantly associated with poor prognosis in patients with HNSCC based on TCGA database (Fig. 9).

Discussion

Accumulating evidence has shown that aberrant expression of miRNAs disrupts the well-ordered RNA networks in cancer cells and is involved in the pathogenesis of human cancers (22). Based on the miRNA expression signatures of human cancers, we have sequentially identified antitumor miRNAs that regulate novel cancer networks (16,23-26). Analyses of our miRNA signature of HNSCC by RNA sequencing showed that several passenger strands of miRNAs were significantly downregulated in cancer tissues (8). Our recent study demonstrated that both strands of pre-*miR-150* (*miR-150-5p*, guide strand; and *miR-150-3p*, passenger strand) had antitumor functions and that these miRNAs cooperatively regulated oncogenic *ITGA3*, *ITGA6* and *TNC* in HNSCC cells (8). Our other studies showed that the passenger strand of *miR-150* acted as an antitumor miRNA in several types of cancers, such as esophageal cancer and prostate cancer (9,27). These findings suggested that miRNA passenger strands also contribute substantially to cancer pathogenesis and that identification of RNA networks mediated by miRNA passenger strands may provide novel insights into the pathogenesis of HNSCC.

Based on our miRNA signature of HNSCC, we focused on the passenger strand *miR-145-3p* in this study. Similarly,

Table III. Identification of *MYO1B* downstream genes in HNSCC cells.

Gene symbol	Gene name	Log_2 (si-*MYO1B*-1/ mock)	Log_2 (si-*MYO1B*-2/ mock)	Average Log_2 (si-*MYO1B*/ mock)
MYO1B	Myosin IB	-4.007414	-4.668526	-4.337970
ANXA10	Annexin A10	-3.842131	-2.8575826	-3.349857
MATN3	Matrilin 3	-4.224010	-2.0824907	-3.153250
SOHLH1	Spermatogenesis and oogenesis specific basic helix-loop-helix 1	-4.337910	-1.8513346	-3.094622
SMAD1-AS1	SMAD1 antisense RNA 1	-3.191749	-2.902154	-3.046952
KRT6B	Keratin 6B, type II	-3.626921	-2.0426638	-2.834793
KLK13	Kallikrein-related peptidase 13	-3.540325	-1.9546604	-2.747493
PAX6	Paired box 6	-2.130839	-3.0853565	-2.608098
C5orf66-AS1	C5orf66 antisense RNA 1	-2.704701	-2.1148643	-2.409783
PDGFRB	Platelet-derived growth factor receptor, β polypeptide	-2.886416	-1.8465691	-2.366492
HSD17B2	Hydroxysteroid (17-β) dehydrogenase 2	-2.325892	-2.3811436	-2.353518
SP140	SP140 nuclear body protein	-2.470807	-2.1072135	-2.289010
OR9G4	Olfactory receptor, family 9, subfamily G, member 4	-2.296291	-2.1278794	-2.212085
FOXD3-AS1	FOXD3 antisense RNA 1 (head to head)	-1.846461	-2.4128325	-2.129647
MAGEB17	Melanoma antigen family B, 17	-2.394958	-1.7456088	-2.070283
AMDHD1	Amidohydrolase domain containing 1	-2.223687	-1.916799	-2.070243
IGFBP1	Insulin-like growth factor binding protein 1	-2.512259	-1.5926342	-2.052446
MMP1	Matrix metallopeptidase 1 (interstitial collagenase)	-1.821691	-2.2728753	-2.047283
EN1	Engrailed homeobox 1	-1.834606	-2.220468	-2.027537
FGF13-AS1	FGF13 antisense RNA 1	-2.349053	-1.6906263	-2.019840
ZC3H12D	Zinc finger CCCH-type containing 12D	-2.232335	-1.8071643	-2.019749
KRT6A	Keratin 6A, type II	-2.307169	-1.6317264	-1.969448
FAM196B	Family with sequence similarity 196, member B	-1.855253	-2.031945	-1.943599
DNMT3B	DNA (cytosine-5-)-methyltransferase 3β	-1.530055	-2.3343146	-1.932185
LIN28A	Lin-28 homolog A (*C. elegans*)	-2.292716	-1.5482489	-1.920483
ZNF501	Zinc finger protein 501	-1.788270	-2.042201	-1.915235
REC114	REC114 meiotic recombination protein	-2.230243	-1.5574937	-1.893868
TRIM9	Tripartite motif containing 9	-2.078308	-1.691343	-1.884826
ZBED3-AS1	ZBED3 antisense RNA 1	-2.140241	-1.6105609	-1.875401
PHKA2-AS1	PHKA2 antisense RNA 1	-2.028810	-1.7067645	-1.867787
ZDHHC22	Zinc finger, DHHC-type containing 22	-2.044774	-1.6702744	-1.857524
SCAND2P	SCAN domain containing 2 pseudogene	-1.924617	-1.7586662	-1.841642
SPRR1B	Small proline-rich protein 1B	-1.967544	-1.7028618	-1.835203
SLC35D3	Solute carrier family 35, member D3	-1.638228	-2.0054185	-1.821823
ANO1-AS2	ANO1 antisense RNA 2 (head to head)	-1.763001	-1.8544457	-1.808723
C22orf23	Chromosome 22 open reading frame 23	-1.741993	-1.8479792	-1.794986
TCTN3	Tectonic family member 3	-1.880425	-1.6976513	-1.789038
FAM198A	Family with sequence similarity 198, member A	-1.940336	-1.6032256	-1.771781
TG	Thyroglobulin	-1.719962	-1.8222181	-1.771090
RASGEF1A	RasGEF domain family, member 1A	-1.865154	-1.6762245	-1.770689
KATNAL2	Katanin p60 subunit A-like 2	-1.982902	-1.5259477	-1.754425
KLHL14	Kelch-like family member 14	-1.575037	-1.9020982	-1.738568
NANOS1	Nanos homolog 1 (*Drosophila*)	-1.785024	-1.6778822	-1.731453
BTBD16	BTB (POZ) domain containing 16	-1.769118	-1.6703396	-1.719729
APOL4	Apolipoprotein L, 4	-1.542360	-1.8804932	-1.711427
ZNF385C	Zinc finger protein 385C	-1.792121	-1.6219425	-1.707032
ABO	ABO blood group	-1.624970	-1.7806495	-1.702810
CD200R1	CD200 receptor 1	-1.778945	-1.5290467	-1.653996
VWA3A	Von Willebrand factor A domain containing 3A	-1.527752	-1.7406074	-1.634180
CYP19A1	Cytochrome P450, family 19, subfamily A, polypeptide 1	-1.572258	-1.6706244	-1.621441
ZNF880	Zinc finger protein 880	-1.604488	-1.6321578	-1.618323
NKX6-2	NK6 homeobox 2	-1.597461	-1.6252115	-1.611336
GPR157	G protein-coupled receptor 157	-1.583724	-1.6133837	-1.598554
ST3GAL5-AS1	ST3GAL5 antisense RNA 1 (head to head)	-1.526179	-1.5542628	-1.540221

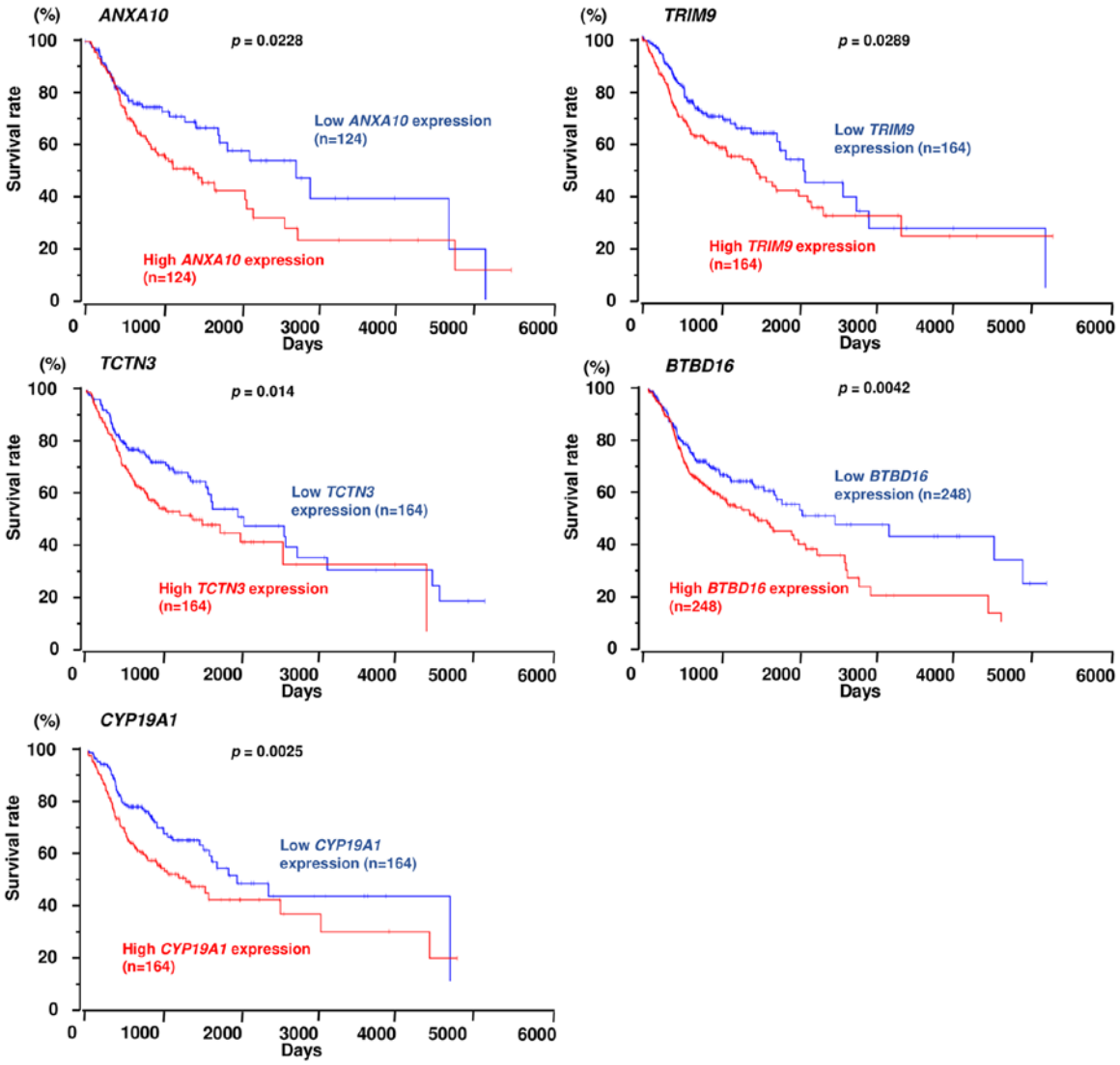

Figure 9. The Cancer Genome Atlas (TCGA) database analysis of myosin 1B (*MYO1B*) downstream genes. Kaplan-Meier survival curve for overall survival with log-rank tests for 5 *MYO1B* downstream genes with high or low expression. TCGA dataset for head and neck squamous cell carcinoma (HNSCC) was analyzed.

miR-145-5p, the guide strand of miR-145, was significantly reduced in this signature. Downregulation of *miR-145-5p* is frequently observed in many types of cancer, and prior studies have confirmed the antitumor function of *miR-145-5p* by demonstration of its effects on several types of oncogenes in cancer cells (10,11). Several studies have shown that down-regulation of *miR-145-5p* is caused by hypermethylation of the promoter region of pre-*miR-145* in prostate cancer (28). Importantly, the tumor suppressor p53 has been shown to directly bind p53-response elements in the promoter region of pre-*miR-145* and to control the expression of *miR-145-5p* (29). p53 mutations are found in >50% of patients with HNSCC (30). Thus, downregulation of *miR-145-5p* and *miR-145-3p* may be dependent on p53 inactivation in cancer cells.

Expression levels of passenger strand of *miR-145-3p* was lower than *miR-145-5p* as a guide strand miRNA in HNSCC clinical specimens and cell lines. Our previous studies of bladder, lung, and prostate cancers showed that expression levels of *miR-145-3p* was lower than *miR-145-5p* in each cancer (10,11,31). The results of the present data of HNSCC was similar to our previous data. Explanation is incomplete as to in what kind of molecular mechanisms the expression of the two miRNAs differ. This problem is an important issue in miRNA biosynthesis.

Our functional assays showed that *miR-145-3p* had antitumor functions similar to *miR-145-5p* in HNSCC cells. We have also demonstrated *miR-145-3p* is downregulated in cancer tissues and acts as an antitumor miRNA in bladder, lung, and prostate cancers by targeting several oncogenic genes (10,11,31). Previous studies demonstrated that several oncogenic genes were regulated by *miR-145-5p* in several types of cancers (32-34). There are few studies for target genes by *miR-145-3p* regulation in cancer cells, including HNSCC cells. Thus, we evaluated *miR-145-3p* regulatory oncogenic networks in HNSCC cells; a total of 14 putative targets of *miR-145-3p* in HNSCC cells were identified in this study. Among these candidates, *MYO1B*, *C16orf74*, *SP9* and *RBP1* were found to be associated with poor prognosis in patients with HNSCC by TCGA data analyses.

In this study, we focused on *MYO1B* because high expression of *MYO1B* was strongly associated with poor prognosis in patients with HNSCC. Myosins are actin-associated

molecular motor proteins that regulate membrane tension, anchor membrane proteins and organelles, and transport intercellular vesicles (35,36). We have demonstrated that antitumor miRNAs inhibited cancer cell migration and invasion through targeting several actin-binding proteins and actin-associate proteins, e.g., FSCN1, LASP1, ARPC5 and ANLN (37-40). Overexpression of these proteins has been detected in cancer tissues and has been shown to contribute to cancer cell aggressiveness.

Our present data of restoration of *miR-145-5p* or *miR-145-3p* showed the inhibition of cancer cell proliferation. However, inhibition of cell proliferation was weak by knockdown of *MYO1B* in HNSCC cells. These data suggest that *miR-145-5p* or *miR-145-3p* inhibite cell proliferation genes and pathways which do not rely on MYO1B in HNSCC cells.

MYO1B belongs to a member of the membrane-associated class I myosin family and functions as a linker between membranes and the actin cytoskeleton in several cellular processes (41). Previous studies have demonstrated other functions of MYO1B. For example, MYO1B is localized in the endocytotic compartment and has pivotal roles in endocytosis (42). MYO1B couples with the actin assembly to organelles and controls membrane remodeling at the trans-Golgi network (43). In cancer cells, *MYO1B* is highly expressed in PC-3 metastatic prostate cancer cells, and knockdown of *MYO1B* affects the cytoskeleton and cell migration (44). Another study showed that knockdown of *MYO1B* significantly inhibits migratory and invasive abilities of HNSCC cells *in vitro* and *in vivo* (35). Our present data confirmed these findings and suggested that MYO1B may be an effective target for the treatment of HNSCC.

To identify MYO1B-mediated HNSCC pathways, we performed genome-wide gene expression analyses using si-*MYO1B* transfectants. A total of 54 genes were found to be mediated by MYO1B in HNSCC. Among them, 5 genes (*ANXA10*, *TRIM9*, *TCTN3*, *BTBD16* and *CYP19A1*) were significantly associated with poor prognosis in patients with HNSCC by TCGA database analyses. Annexin family proteins are calcium-dependent phospholipid-binding proteins that regulate cell growth and signal transduction (45). Overexpression of *ANXA10* has been reported in oral squamous cell carcinoma, and expression of *ANXA10* promotes cancer cell proliferation through regulating mitogen-activated protein kinase signaling pathways (46). Exploration of novel *MYO1B*-mediated pathways may improve our understanding of the aggressiveness of this disease.

In conclusion, downregulation of *miR-145-3p* was observed in HNSCC clinical specimens, and this passenger strand acted as an antitumor miRNA through targeting *MYO1B* in HNSCC cells. *MYO1B* was highly expressed in HNSCC clinical specimens and was found to promote cancer aggressiveness in functional assays. Elucidation of the pathways mediated by the *miR-145-3p*/*MYO1B* axis is expected to contribute to further analyses of oncogenesis mechanisms and treatment strategies in HNSCC.

Acknowledgements

This study was supported by JSPS KAKENHI (grant nos. 17K16893, 16K20229, 15K10801, 16K11224 and 17K11375).

References

1. Jemal A, Siegel R, Xu J and Ward E: Cancer statistics, 2010. CA Cancer J Clin 60: 277-300, 2010.
2. Jou A and Hess J: Epidemiology and molecular biology of head and neck cancer. Oncol Res Treat 40: 328-332, 2017.
3. Sawicki M, Szudy A, Szczyrek M, Krawczyk P and Klatka J: Molecularly targeted therapies in head and neck cancers. Otolaryngol Pol 66: 307-312, 2012.
4. Bartel DP: MicroRNAs: Genomics, biogenesis, mechanism, and function. Cell 116: 281-297, 2004.
5. Filipowicz W, Bhattacharyya SN and Sonenberg N: Mechanisms of post-transcriptional regulation by microRNAs: Are the answers in sight? Nat Rev Genet 9: 102-114, 2008.
6. Adams BD, Kasinski AL and Slack FJ: Aberrant regulation and function of microRNAs in cancer. Curr Biol 24: R762-R776, 2014.
7. Mah SM, Buske C, Humphries RK and Kuchenbauer F: miRNA*: A passenger stranded in RNA-induced silencing complex? Crit Rev Eukaryot Gene Expr 20: 141-148, 2010.
8. Koshizuka K, Nohata N, Hanazawa T, Kikkawa N, Arai T, Okato A, Fukumoto I, Katada K, Okamoto Y and Seki N: Deep sequencing-based microRNA expression signatures in head and neck squamous cell carcinoma: Dual strands of pre-miR-150 as antitumor miRNAs. Oncotarget 8: 30288-30304, 2017.
9. Okato A, Arai T, Kojima S, Koshizuka K, Osako Y, Idichi T, Kurozumi A, Goto Y, Kato M, Naya Y, *et al*: Dual strands of pre-miR-150 (miR-150-5p and miR-150-3p) act as antitumor miRNAs targeting SPOCK1 in naïve and castration-resistant prostate cancer. Int J Oncol 51: 245-256, 2017.
10. Mataki H, Seki N, Mizuno K, Nohata N, Kamikawaji K, Kumamoto T, Koshizuka K, Goto Y and Inoue H: Dual-strand tumor-suppressor microRNA-145 (miR-145-5p and miR-145-3p) coordinately targeted MTDH in lung squamous cell carcinoma. Oncotarget 7: 72084-72098, 2016.
11. Matsushita R, Yoshino H, Enokida H, Goto Y, Miyamoto K, Yonemori M, Inoguchi S, Nakagawa M and Seki N: Regulation of UHRF1 by dual-strand tumor-suppressor microRNA-145 (miR-145-5p and miR-145-3p): Inhibition of bladder cancer cell aggressiveness. Oncotarget 7: 28460-28487, 2016.
12. Matsushita R, Seki N, Chiyomaru T, Inoguchi S, Ishihara T, Goto Y, Nishikawa R, Mataki H, Tatarano S, Itesako T, *et al*: Tumour-suppressive microRNA-144-5p directly targets CCNE1/2 as potential prognostic markers in bladder cancer. Br J Cancer 113: 282-289, 2015.
13. Yonemori M, Seki N, Yoshino H, Matsushita R, Miyamoto K, Nakagawa M and Enokida H: Dual tumor-suppressors miR-139-5p and miR-139-3p targeting matrix metalloprotease 11 in bladder cancer. Cancer Sci 107: 1233-1242, 2016.
14. Karatas OF, Yuceturk B, Suer I, Yilmaz M, Cansiz H, Solak M, Ittmann M and Ozen M: Role of miR-145 in human laryngeal squamous cell carcinoma. Head Neck 38: 260-266, 2016.
15. Huang SH and O'Sullivan B: Overview of the 8th edition TNM classification for head and neck cancer. Curr Treat Options Oncol 18: 40, 2017.
16. Fukumoto I, Hanazawa T, Kinoshita T, Kikkawa N, Koshizuka K, Goto Y, Nishikawa R, Chiyomaru T, Enokida H, Nakagawa M, *et al*: MicroRNA expression signature of oral squamous cell carcinoma: Functional role of microRNA-26a/b in the modulation of novel cancer pathways. Br J Cancer 112: 891-900, 2015.
17. Koshizuka K, Hanazawa T, Fukumoto I, Kikkawa N, Matsushita R, Mataki H, Mizuno K, Okamoto Y and Seki N: Dual-receptor (EGFR and c-MET) inhibition by tumor-suppressive miR-1 and miR-206 in head and neck squamous cell carcinoma. J Hum Genet 62: 113-121, 2017.
18. Nohata N, Sone Y, Hanazawa T, Fuse M, Kikkawa N, Yoshino H, Chiyomaru T, Kawakami K, Enokida H, Nakagawa M, *et al*: miR-1 as a tumor suppressive microRNA targeting TAGLN2 in head and neck squamous cell carcinoma. Oncotarget 2: 29-42, 2011.
19. Goto Y, Kojima S, Nishikawa R, Enokida H, Chiyomaru T, Kinoshita T, Nakagawa M, Naya Y, Ichikawa T and Seki N: The microRNA-23b/27b/24-1 cluster is a disease progression marker and tumor suppressor in prostate cancer. Oncotarget 5: 7748-7759, 2014.
20. Arai T, Okato A, Kojima S, Idichi T, Koshizuka K, Kurozumi A, Kato M, Yamazaki K, Ishida Y, Naya Y, *et al*: Regulation of spindle and kinetochore-associated protein 1 by antitumor miR-10a-5p in renal cell carcinoma. Cancer Sci 108: 2088-2101, 2017.

21. Kurozumi A, Goto Y, Matsushita R, Fukumoto I, Kato M, Nishikawa R, Sakamoto S, Enokida H, Nakagawa M, Ichikawa T, *et al*: Tumor-suppressive microRNA-223 inhibits cancer cell migration and invasion by targeting ITGA3/ITGB1 signaling in prostate cancer. Cancer Sci 107: 84-94, 2016.
22. Esquela-Kerscher A and Slack FJ: Oncomirs - microRNAs with a role in cancer. Nat Rev Cancer 6: 259-269, 2006.
23. Nohata N, Hanazawa T, Kikkawa N, Sakurai D, Fujimura L, Chiyomaru T, Kawakami K, Yoshino H, Enokida H, Nakagawa M, *et al*: Tumour suppressive microRNA-874 regulates novel cancer networks in maxillary sinus squamous cell carcinoma. Br J Cancer 105: 833-841, 2011.
24. Fukumoto I, Kinoshita T, Hanazawa T, Kikkawa N, Chiyomaru T, Enokida H, Yamamoto N, Goto Y, Nishikawa R, Nakagawa M, *et al*: Identification of tumour suppressive microRNA-451a in hypopharyngeal squamous cell carcinoma based on microRNA expression signature. Br J Cancer 111: 386-394, 2014.
25. Goto Y, Kojima S, Nishikawa R, Kurozumi A, Kato M, Enokida H, Matsushita R, Yamazaki K, Ishida Y, Nakagawa M, *et al*: MicroRNA expression signature of castration-resistant prostate cancer: The microRNA-221/222 cluster functions as a tumour suppressor and disease progression marker. Br J Cancer 113: 1055-1065, 2015.
26. Goto Y, Kurozumi A, Nohata N, Kojima S, Matsushita R, Yoshino H, Yamazaki K, Ishida Y, Ichikawa T, Naya Y, *et al*: The microRNA signature of patients with sunitinib failure: Regulation of UHRF1 pathways by microRNA-101 in renal cell carcinoma. Oncotarget 7: 59070-59086, 2016.
27. Osako Y, Seki N, Koshizuka K, Okato A, Idichi T, Arai T, Omoto I, Sasaki K, Uchikado Y, Kita Y, *et al*: Regulation of SPOCK1 by dual strands of pre-miR-150 inhibit cancer cell migration and invasion in esophageal squamous cell carcinoma. J Hum Genet: Jun 29, 2017. (Epub ahead of print). doi: 10.1038/jhg.2017.69.
28. Xia W, Chen Q, Wang J, Mao Q, Dong G, Shi R, Zheng Y, Xu L and Jiang F: DNA methylation mediated silencing of microRNA-145 is a potential prognostic marker in patients with lung adenocarcinoma. Sci Rep 5: 16901, 2015.
29. Yang P, Yang Y, An W, Xu J, Zhang G, Jie J and Zhang Q: The long noncoding RNA-ROR promotes the resistance of radiotherapy for human colorectal cancer cells by targeting the p53/miR-145 pathway. J Gastroenterol Hepatol 32: 837-845, 2017.
30. Wood NB, Kotelnikov V, Caldarelli DD, Hutchinson J, Panje WR, Hegde P, Leurgans S, LaFollette S, Taylor SG IV, Preisler HD, *et al*: Mutation of p53 in squamous cell cancer of the head and neck: Relationship to tumor cell proliferation. Laryngoscope 107: 827-833, 1997.
31. Goto Y, Kurozumi A, Arai T, Nohata N, Kojima S, Okato A, Kato M, Yamazaki K, Ishida Y, Naya Y, *et al*: Impact of novel miR-145-3p regulatory networks on survival in patients with castration-resistant prostate cancer. Br J Cancer 117: 409-420, 2017.
32. Pashaei E, Guzel E, Ozgurses ME, Demirel G, Aydin N and Ozen M: A Meta-analysis: Identification of common mir-145 target genes that have similar behavior in different GEO datasets. PLoS One 11: e0161491, 2016.
33. Sachdeva M and Mo YY: miR-145-mediated suppression of cell growth, invasion and metastasis. Am J Transl Res 2: 170-180, 2010.
34. Das AV and Pillai RM: Implications of miR cluster 143/145 as universal anti-oncomiRs and their dysregulation during tumorigenesis. Cancer Cell Int 15: 92, 2015.
35. Ohmura G, Tsujikawa T, Yaguchi T, Kawamura N, Mikami S, Sugiyama J, Nakamura K, Kobayashi A, Iwata T, Nakano H, *et al*: Aberrant myosin 1b expression promotes cell migration and lymph node metastasis of HNSCC. Mol Cancer Res 13: 721-731, 2015.
36. Salas-Cortes L, Ye F, Tenza D, Wilhelm C, Theos A, Louvard D, Raposo G and Coudrier E: Myosin Ib modulates the morphology and the protein transport within multi-vesicular sorting endosomes. J Cell Sci 118: 4823-4832, 2005.
37. Fuse M, Nohata N, Kojima S, Sakamoto S, Chiyomaru T, Kawakami K, Enokida H, Nakagawa M, Naya Y, Ichikawa T, *et al*: Restoration of miR-145 expression suppresses cell proliferation, migration and invasion in prostate cancer by targeting FSCN1. Int J Oncol 38: 1093-1101, 2011.
38. Nishikawa R, Goto Y, Sakamoto S, Chiyomaru T, Enokida H, Kojima S, Kinoshita T, Yamamoto N, Nakagawa M, Naya Y, *et al*: Tumor-suppressive microRNA-218 inhibits cancer cell migration and invasion via targeting of LASP1 in prostate cancer. Cancer Sci 105: 802-811, 2014.
39. Kinoshita T, Nohata N, Watanabe-Takano H, Yoshino H, Hidaka H, Fujimura L, Fuse M, Yamasaki T, Enokida H, Nakagawa M, *et al*: Actin-related protein 2/3 complex subunit 5 (ARPC5) contributes to cell migration and invasion and is directly regulated by tumor-suppressive microRNA-133a in head and neck squamous cell carcinoma. Int J Oncol 40: 1770-1778, 2012.
40. Idichi T, Seki N, Kurahara H, Yonemori K, Osako Y, Arai T, Okato A, Kita Y, Arigami T, Mataki Y, *et al*: Regulation of actin-binding protein ANLN by antitumor miR-217 inhibits cancer cell aggressiveness in pancreatic ductal adenocarcinoma. Oncotarget 8: 53180-53193, 2017.
41. Yamada A, Mamane A, Lee-Tin-Wah J, Di Cicco A, Prévost C, Lévy D, Joanny JF, Coudrier E and Bassereau P: Catch-bond behaviour facilitates membrane tubulation by non-processive myosin 1b. Nat Commun 5: 3624, 2014.
42. Komaba S and Coluccio LM: Localization of myosin 1b to actin protrusions requires phosphoinositide binding. J Biol Chem 285: 27686-27693, 2010.
43. Almeida CG, Yamada A, Tenza D, Louvard D, Raposo G and Coudrier E: Myosin 1b promotes the formation of post-Golgi carriers by regulating actin assembly and membrane remodelling at the trans-Golgi network. Nat Cell Biol 13: 779-789, 2011.
44. Makowska KA, Hughes RE, White KJ, Wells CM and Peckham M: Specific myosins control actin organization, cell morphology, and migration in prostate cancer cells. Cell Rep 13: 2118-2125, 2015.
45. Qi H, Liu S, Guo C, Wang J, Greenaway FT and Sun MZ: Role of annexin A6 in cancer. Oncol Lett 10: 1947-1952, 2015.
46. Shimizu T, Kasamatsu A, Yamamoto A, Koike K, Ishige S, Takatori H, Sakamoto Y, Ogawara K, Shiiba M, Tanzawa H, *et al*: Annexin A10 in human oral cancer: Biomarker for tumoral growth via G1/S transition by targeting MAPK signaling pathways. PLoS One 7: e45510, 2012.